HHS Public Access

Author manuscript

J Neuroendocrinol. Author manuscript; available in PMC 2022 August 01.

Published in final edited form as:

J Neuroendocrinol. 2021 August ; 33(8): e13006. doi:10.1111/jne.13006.

Neuropeptide Y suppresses thermogenic and cardiovascular sympathetic nerve activity via Y1 receptors in the paraventricular nucleus and dorsomedial hypothalamus

Zhigang Shi[#1], **Alyssa C. Bonillas**[#1], **Jennifer Wong**[1], **Stephanie L. Padilla**[2], **Virginia L. Brooks**[1]

[1]Department of Chemical Physiology and Biochemistry, Oregon Health & Science University, Portland, OR, USA 97239

[2]Department of Biology, University of Massachusetts, Amherst, Amherst, MA, USA 01003

[#] These authors contributed equally to this work.

Abstract

In hungry animals, Neuropeptide Y (NPY) neurons in the arcuate nucleus (ArcN) are activated to suppress energy expenditure, in part by decreasing brown adipose tissue sympathetic nerve activity (BAT SNA); however, the NPY receptor subtype and brain neurocircuitry are unclear. Here, we investigated the inhibition of BAT SNA by exogenous and endogenous NPY via binding to Y1 receptors (NPY1R) in the hypothalamic paraventricular nucleus (PVN) and dorsomedial hypothalamus (DMH), in anesthetized male rats. Downstream projections of PVN/DMH NPY1R-expressing neurons were identified using male *npy1r-cre* mice and localized unilateral DMH or PVN injections of an adeno-associated virus (AAV), which allows for the cre-dependent expression of a fluorescent protein (mCherry) in the cell bodies, axon fibers, and nerve terminals of NPY1R-containing neurons. Nanoinjections of NPY into the DMH of cooled rats decreased BAT SNA, as well as mean arterial pressure (MAP) and heart rate (HR), and these responses were reversed by subsequent injection of the selective NPY1R antagonist, BIBO3304. In warmed rats, with little to no BAT SNA, bilateral nanoinjections of BIBO3304 into the DMH or PVN increased BAT SNA, MAP, and HR. DMH NPY1R-expressing neurons projected heavily to the Raphe Pallidus (RPa), which houses BAT presympathetic neurons, as well as the PVN. In anesthetized mice, DMH BIBO3304 increased splanchnic SNA, MAP, and HR, all of which were reversed by nonselective blockade of the PVN with muscimol, suggesting that DMH-to-PVN connections are involved in this DMH BIBO3304 disinhibition. PVN Y1R expressing neurons also projected to the RPa, as well as to the nucleus tractus solitarius. We conclude that NPY tonically released in the

Correspondence: Virginia L. Brooks, Ph.D., Department of Chemical Physiology and Biochemistry, Oregon Health & Science University, 3181 SW Sam Jackson Park Rd, Portland, OR 97239, brooksv@ohsu.edu, 503-494-5843, FAX: 503-494-435.

AUTHOR CONTRIBUTIONS:

- conception or design of the work: zs, ab, vlb
- acquisition, analysis or interpretation of data for the work: zs, ab, jw, nep, slp, vlb
- drafting the work or revising it critically for important intellectual content: zs, ab, jw, nep, slp, vlb

CONFLICT OF INTEREST:

The authors have no conflicts of interest to declare.

DMH and PVN suppresses BAT SNA, MAP, and HR via Y1R. Downstream neuropathways for BAT SNA may utilize direct projections to the RPa. Release of tonic NPY inhibition of BAT SNA may contribute to feeding- and diet-induced thermogenesis.

Article Summary:

NPY tonically released in the DMH and PVN suppresses BAT SNA via Y1 receptors and neuropathways that may utilize direct projections to the RPa. Release of this tonic NPY inhibition may contribute to feeding- and diet-induced thermogenesis.

Keywords

brown adipose tissue sympathetic nerve activity; Neuropeptide Y; paraventricular nucleus; dorsomedial hypothalamus; Y1 receptor

INTRODUCTION

Energy homeostasis is maintained through regulation of the balance between food intake and energy expenditure, which in turn is determined by the basal metabolic rate, activity, and thermogenesis. Energy balance is controlled chiefly by the hypothalamus, and the arcuate nucleus (ArcN) is pivotal in this regulation. In hungry animals, ArcN Neuropeptide Y (NPY) neurons are activated by ghrelin to stimulate food intake and suppress energy expenditure via inhibition of basal metabolic rate, suppression of the hypothalamic pituitary thyroid (HPT) axis, and inhibition of thermogenesis (1–3). NPY also suppresses heat production in cooled animals via a decrease in brown adipose tissue (BAT) sympathetic nerve activity (SNA). Conversely, the increase in thermogenesis induced by refeeding or overfeeding depends on NPY suppression (4, 5).

The brain neurocircuity by which NPY controls BAT SNA is incompletely understood. Major targets of ArcN NPY neurons in the control of food intake and SNA are the hypothalamic paraventricular nucleus (PVN) and the dorsomedial hypothalamus (DMH) (6, 7). Considerable evidence implicates NPY-receptive PVN neurons in the control of BAT. Nanoinjections of NPY into the PVN decrease BAT SNA, BAT UCP1, and thermogenesis in cooled rodents (8, 9). Moreover, select restoration of NPY only in the ArcN of NPY null mice decreases energy expenditure, BAT temperature, and BAT UCP1 expression via a neuropathway that includes the PVN (2). The circuitry downstream of the PVN ultimately suppresses activity of BAT presympathetic neurons housed in the rostral Raphe Pallidus (RPa), which also serves as an integrating center for various modalities influencing the activity of BAT SNA and thermogenesis, like a change in body temperature or a fever (10). A recent report (11) suggests that NPY in the PVN inhibits BAT SNA by activating GABAergic neurons in the medullary intermediate and parvicellular reticular nuclei (IRt/PCRt) that project to the RPa.

The DMH is another well-established node in the brain circuitry by which both cooling and a fever activate BAT thermogenesis (10). However, whether NPY projections to the DMH also suppress BAT SNA and temperature has not been previously investigated. Therefore,

we first tested if NPY nanoinjections into the DMH decreases BAT SNA, in rats cooled to elevate ongoing BAT SNA. The NPY receptor subtype that mediates the suppression of BAT SNA by NPY is also unclear. The action of ArcN NPY to suppress BAT UCP1 expression was mediated by the Y1R, but not the Y2R (2). In parallel, NPY1R in the PVN also mediates the effect of select chemogenetic activation of ArcN NPY neurons to increase food intake (6). However, whether NPY binds to Y1R in the DMH to inhibit BAT SNA or whether endogenous NPY tonically suppresses BAT SNA via the Y1R in either PVN or DMH is unknown. Therefore, we next tested if nanoninjections of the select Y1R antagonist, BIBO3304, into the PVN or DMH increases BAT SNA in warmed rats. Finally, we surveyed projection targets of DMH and PVN Y1R containing neurons, using male *Npy1r-cre* mice and localized unilateral DMH or PVN injections of an adeno-associated virus (AAV), which allows for the cre-dependent expression of a fluorescent protein (mCherry) in the cell bodies, axon fibers, and nerve terminals of NPY1R-containing neurons.

MATERIALS AND METHODS.

Animals.

All procedures were conducted in accordance with the National Institutes of Health Guide for the Care and Use of Laboratory Animals and approved by the Institutional (Oregon Health & Science University) Animal Care and Use Committee.

Rats.—Male Sprague-Dawley rats (Charles River; 350–450 g) were used. All rats were acclimated for ≥1 week before experimentation in a room with a 12:12-h light/dark cycle, with ambient temperature maintained at 22±1 °C, and with food (LabDiet 5001, Richmond, IN) and water provided ad libitum.

Mice.—A *Npy1r*$^{Cre:GFP}$ knock-in mouse line was provided by Dr. Richard Palmiter (Jackson 030544), in which Cre recombinase is driven off of the regulatory elements of the *Npy1r* gene and is inserted upstream of initiation codon of the endogenous gene to induce specific expression of mCherry in NPY1R containing cells (12). This specific expression was confirmed here as follows: Isoflurane anesthetized mice received unilateral injections of ≤10 nL of AAV8.2-hEF1alpha-DIO-Synaptophysin-mCherry-WPRE (VIROVEK, CA; AAV-Syn-mCherry) into the PVN (see below). After recovery, the mice were deeply anesthetized with Euthasol and perfused with 4% paraformaldehyde. The brains were removed, post-fixed for 6 hr, and sectioned. Combined RNAScope *in situ* hybridization for *Npyr1* and immunohistochemistry (ihc) for mCherry were then conducted as previously described (13). As shown in Figure 1, the vast majority of mCherry neurons expressed NPY1R mRNA.

AgRP-ires-Cre mice were originally obtained from Jackson Labs and were bred and genotyped in house.

Role of DMH and PVN NPY Y1R to inhibit BAT SNA.

Surgery.—Rats were anesthetized with isoflurane and prepared for DMH and PVN nanoinjections, and for measurements of BAT SNA, BAT temperature, mean and pulsatile

arterial pressure (MAP and AP), and heart rate (HR) as previously described (13–15). When surgery was completed, rats were transitioned to α-chloralose anesthesia (Sigma; 50 mg/kg loading dose followed by 25 mg/kg hr continuous infusion for the duration of the experiment), while slowly withdrawing the isoflurane over 30 min. A water-perfused thermal blanket was used to maintain skin and body temperature close to 37°C. During a 1 hr stabilization period, expired CO_2 was continuously recorded and maintained at 30–40 mmHg via artificial ventilation and by adjusting the respiratory rate (60–80 bpm) and tidal volume (1 ml/ 100 g BW; 3.5–4.5 ml) of 100% oxygen.

Hypothalamic nanoinjections.—With the skull secured in a flat position in a stereotaxic device, and using bregma and the dural surface as zero, nanoinjections were made into the DMH (3.2, caudal; 0.5, lateral; and 8.3–8.8, ventral) or PVN (1.7–1.9 mm caudal, 0.5 mm lateral and 7.3–7.5 mm ventral). All nanoinjections (60 nl) were made bilaterally, with ~2 min between injections, and each injection was conducted over approximately 5–10 s using a pressure injection system (Pressure System IIe, Toohey Company, Fairfield, NJ, USA). Fluorescent polystyrene microspheres (Fluo-Spheres, F8803, 1:200; Molecular Probes, Eugene OR) were included in the injectate to verify the injection sites. Drugs for nanoinjections were dissolved in artificial cerebrospinal fluid (aCSF) containing (in mM): 128 NaCl, 2.6 KCl, 1.3 $CaCl_2$, 0.9 $MgCl_2$, 20 $NaHCO_3$, 1.3 Na_2HPO_4 and 2 dextrose; pH 7.4.

Experimental Protocols.—1. *Does NPY in the DMH inhibit BAT SNA in cooled rats by binding to Y1R?* To cool the rats, body temperature was allowed to fall over about 1 hr by eliminating heat emanating from the blanket and pad. Experiments were initiated when body temperature was stable at ~35.5°C for more than 30 min. After stabilization, NPY (60 nL of 0.1 mmol/l) was injected bilaterally into the DMH. After 15 min, the highly selective NPY Y1R antagonist, BIBO3304 (60 nL of 1mmol/l), was injected bilaterally into the DMH. Data collection continued for another 30 min. 2. *Does endogenous NPY tonically inhibit BAT SNA via Y1R in the DMH and PVN?* In separate groups of warmed animals, BIBO3304 (60 nL of 1 mmol/l) was nanoinjected bilaterally into the PVN or DMH, and data were collected for 30 min.

Data acquisition.—MAP, AP, HR, BAT temperature, and raw BAT SNA were continuously recorded throughout the experiment with Grass amplifiers (Model 79D, Grass Instrument Co., Quincy, MA, USA) and a Biopac MP100 data acquisition and analysis system (Biopac Systems, Inc., Santa Barbara, CA, USA), sampling at 2000 Hz. BAT SNA was band-pass filtered (20–3000 Hz) and amplified (×10,000). The SNA signal was then rectified and integrated in 1-s bins. After the experiment, rats were euthanized with an overdose of pentobarbital, and background post-mortem BAT SNA was subtracted from values of BAT SNA recorded during the experiment. BAT SNA was normalized to the baseline (or control) SNA, which was defined as the average of the 30 sec period before the first injection and expressed as percentage of control (% Control).

Data analysis and statistics.—All data were grouped into 1-min bins and averaged; baseline was the 1-min average before the first bilateral nanoinjection. Data used for

statistical analysis in Figures 2 and 7 were collected as follows: the first experimental point (Figure 2 NPY and Figure 7 Y1x) was the 1-min average just before the second bilateral injections. The second experimental point (Figure 2 BIBO3304 and Figure 7 muscimol) was the peak response (of 1-min averages) following the injection.

One-way or two-way ANOVA for repeated measures was conducted using the statistical program GB-STAT (Dynamic Microsystems, Inc.). Specific within and between group differences were determined using the post-hoc Newman-Keuls test. In two cases (BAT SNA after PVN or DMH BIBO3304), data were non-normal, so were log-transformed to normalize before ANOVA analysis. $P<0.05$ was considered statistically significant.

Downstream projection targets of DMH and PVN Y1R-expressing neurons.

Stereotaxic AAV-Syn-mCherry injections into the DMH and PVN.—Under isoflurane (1.5%–2.5%) anesthesia, ≤10 nL of AAV-Syn-mCherry (to label cell bodies, axons, and nerve terminals) were injected unilaterally into the DMH [coordinates: 1.7 mm caudal to bregma; 5.1 mm ventral from dura; ± 0.4 mm lateral from midline] or PVN (coordinates: 0.9 mm caudal to bregma; 4.8 mm ventral from dura; ±0.3 mm lateral to midline). Mice were allowed to recover for a minimum of 2 weeks prior to being sacrificed with an overdose of barbituates. The brains were then removed and fixed in 4% paraformaldehyde overnight and transferred to 20% sucrose solution.

Stereotaxic AAV-Syn-mCherry injections into the ARC.—To determine if NPY that binds to DMH Y1R originates from neurons in the ArcN, we identified ArcN BAT pre-sympathetic neurons by injecting the retrogradely transported indicator Cholera toxin B (CtB; Alexa-488-CtB 1mg/ml, 30 nL, Life Technologies, Invitrogen™, Carlsbad, CA) into the RPa (7). Using the Cre-dependent synaptically-targeted AAV-Syn-mCherry injected bilaterally into the ArcN (coordinates: 1.0 to 1.6 mm caudal to bregma, 0.3 mm lateral to midline, 5.8 mm ventral to dura) of *AgRP-ires-Cre* mice, confocal microscopy (LSM 880indimo AxioObserver with 63x/1.4 Oil immersion objective imaging 16–5 μm optical sections), and ZenBlue software, we tested if DMH CtB labeled neurons are closely associated with ArcN NPY/AgRP neuronal terminals.

Immunohistochemistry: Mouse brains were frozen and sectioned at 40 μm for immunohistochemical processing to detect the presence of mCherry-labeled neurons, axon fibers, and nerve endings. Sections were treated with rabbit anti-mCherry (1:1000; ab167453, Abcam) primary antibody, then Alexa Fluor 594–donkey anti-rabbit (1:1000; catalog A21207, Invitrogen). Sections were mounted with Prolong Gold + DAPI nuclear stain to enhance anatomical identifications.

The role of the PVN in sympathoinhibitory actions of NPY in the DMH.—We previously reported that NPY released from ArcN neuronal projections to the DMH tonically suppresses Splanchnic SNA (SSNA) (7). However, the downstream neurocircuitry is unknown. Because DMH neurons send a major projection to the PVN, we determined if DMH Y1R-expressing neurons are among this population (above) and also tested if nonspecific blockade of the PVN reverses the sympathoexcitatory effects of blockade of

DMH Y1R. Wild-type mice were prepared for hypothalamic nanoinjections as previously described (7). Briefly, mice were anesthetized with 1.5–2.5% isoflurane in 100% oxygen. The mice were intubated to allow for spontaneous respiration of oxygen-enriched room air; rectal temperature was maintained at 36–38°C using a rectal thermistor and heating pad. A bipolar stainless steel electrode was implanted around the splanchnic nerve, the right jugular vein was cannulated to maintain anesthesia after surgery with α-chloralose (initial dose: 25 mg/kg; sustaining dose of 6 mg/kg/hr, Sigma-Aldrich, St. Louis, MO), the left carotid artery was cannulated for continuous measurement of AP and HR, and the skull was cleared and prepared for nanoinjections by burring a hole in the skull near the midline. After surgery and the α-chloralose loading dose, mice were allowed to stabilize for ≥30 min before experimentation. We first bilaterally injected the selective NPY1R antagonist, BIBO3304 (30 nl of 10 mmol/l; Tocris Bioscience), into the DMH (coordinates: 1.7–1.9 mm caudal, 0.4 mm lateral and 5.1 mm ventral to bregma/dura). After 15 min, the inhibitory $GABA_A$ agonist, muscimol (30 nL of 1 mmol/l; Tocris Bioscience), was injected bilaterally into the PVN (coordinates: 0.7–0.9 mm caudal, 0.3–0.4 mm lateral and 4.8 mm ventral to bregma/dura). All injectates were dissolved in aCSF and included fluorescent polystyrene microspheres (Fluo-Spheres, F8803, 1:200) to verify injection sites. After experimentation, all mice were killed with an overdose of pentobarbital. The post-mortem nerve activity was recorded and subtracted from experimental values of SSNA and normalized to baseline (average of 60 sec before the first injection). Data were grouped into 1-min bins, averaged, and between treatment differences ($P<0.05$) were determined using 1-way repeated measures ANOVA and the post-hoc-Newman Keuls test.

RESULTS.

DMH NPY inhibits BAT SNA via Y1R.

Bilateral injections of NPY into the DMH of cooled rats (35.6±0.1°C) promptly decreased BAT SNA, BAT T, expired CO_2, as well as MAP and HR (Figure 2). These decreases were rapidly reversed by injection of the selective Y1R antagonist, BIBO3304, into the DMH. Indeed, both BAT SNA and BAT T were elevated above basal levels, suggesting that BIBO3304 was not only reversing the effects of exogenous NPY, but also the inhibition mediated by tonically released endogenous NPY. Thus, NPY can bind to NPY1R in the DMH to suppress BAT SNA, which decreases BAT T and expired CO_2.

Endogenous NPY suppresses BAT SNA by binding to Y1R in the DMH and PVN.

To specifically test if endogenous NPY tonically suppresses basal BAT SNA via Y1R, we next injected BIBO3304 into the DMH, as well as into the PVN, of warmed rats (37.0±0.1°C) with little to no ongoing BAT SNA. As shown by both representative experiments (Figures 3 and 4, left panel) and grouped data (Figures 3 and 4, right panel), BIBO3304 injections into both the DMH (Figure 3) and PVN (Figure 4) increased BAT SNA, BAT T, and CO_2, as well as MAP and HR. Thus, NPY tonically released in the DMH and PVN inhibits BAT SNA via binding to NPY Y1R. Injection sites are illustrated in Figure 5.

DMH Y1R expressing neurons send projections to PVN and RPa.

Of the 7 mice that received viral vector injections into the DMH, in three cases the injections induced neuronal cell body mCherry expression selectively restricted to the DMH (Figures 6A and 6B). Within the hypothalamus, fibers and nerve endings were extensively distributed within the PVN (Figures 6C and 6D), as well as a lighter distribution within the ArcN (Figure 6E). As previously shown (7), blockade of DMH Y1R increases SSNA in mice (Figure 7A, representative experiment; 7B, grouped data). The sympathoexcitation was reversed with subsequent nonspecific blockade of the PVN with muscimol (Figures 7A and 7B), indicating that the increase in SSNA elicited by blockade of DMH Y1R depends on the PVN.

As expected, mCherry-labeled fibers and nerve endings from DMH cell bodies were also detected throughout the rostral to caudal RPa (Figure 6F). In addition, in *AgRP-ires-Cre* mice that received AAV-Syn-mCherry into the ArcN to identify ArcN NPY projections to the DMH and also the retrograde tracer CtB into the RPa to identify DMH neurons that project to the RPa, DMH CtB-containing neurons were closely associated with mCherry fibers/nerve endings from ArcN NPY/AgRP neurons (Figure 6G). Thus, the ArcN is likely one source of NPY that inhibits BAT SNA by binding to Y1R in the DMH.

PVN Y1R expressing neurons send projections to the RPa and NTS.

Six mice received AAV-Syn-mCherry injections directed at the PVN; in 3 mice the injections were well placed, as shown in a representative mouse (Figure 8A). Interestingly, as with mice that received DMH mCherry AAV, the mCherry signal was observed in rostral through caudal levels of the RPa (Figures 8B–D). Intense projections were also observed in the NTS and area postrema (Figures 9A–D).

Using CtB to label PVN neurons that project to the RVLM coupled with ihc using an antibody directed against the NPY Y1R, we previously demonstrated that, in rats, NPY Y1R-expressing PVN neurons project to the RVLM (16). In the present study, projections of PVN NPY Y1R-expressing neurons were instead visualized using *Npy1r cre* mice that received mCherry-Syn-AAV. In these mice, fibers in RVLM were apparent but limited (Figure 10A). Instead, a marked cluster of fibers and nerve endings were observed in the presumed caudal pressor area (Figure 10B), another pre-sympathetic site well described in the rat (17, 18).

DISCUSSION.

Activated ArcN NPY neurons, as with hunger, stimulate feeding and inhibit the sympathetic nervous system (1, 7). Conversely, decreases in NPY contribute to satiation and likely diet- or feeding-induced thermogenesis. Indirect support for the latter includes the findings that refeeding of fasted animals triggers an anticipatory decrease in ArcN NPY neuronal activity (19) and, in parallel, activates BAT (20). While considerable information has identified the situations and downstream effectors of NPY-induced feeding, much less is known about the central actions of NPY on neural control of BAT. Given the recent renaissance of energy-releasing BAT in the control of body weight, this information is critical. The goal

of this study was to further delineate the neurocircuitry by which NPY decreases BAT SNA and BAT temperature and to test if tonically released endogenous NPY suppresses BAT SNA via Y1R in the DMH and PVN. The important new findings are that: 1) DMH NPY dramatically suppresses BAT SNA in cooled rats, and this effect can be reversed with the select NPY Y1R antagonist, BIBO3304. 2) In warmed rats, with little to no ongoing BAT SNA, bilateral nanoinjections of BIBO3304 into the DMH or PVN increases BAT SNA. 3) DMH Y1R-expressing neurons project heavily to the RPa and PVN; ArcN NPY/AgRP neuronal fibers closely associate with DMH RPa-projecting neurons, suggesting that the ArcN is at least one source of NPY that influences BAT presympathetic neurons in the DMH. 4) The increase in SSNA elicited by DMH BIBO3304 can be reversed with nonspecific blockade of the PVN. 5) PVN Y1R expressing neurons project to the RPa and NTS/AP. We conclude that NPY tonically released in the DMH and PVN suppresses BAT SNA via Y1R and neuropathways that may utilize direct projections to the RPa.

The DMH is a pivotal link and integrating center in the neuropathways by which fever and cooling activate BAT (10). In the context of energy balance, leptin and MC4Rs in the DMH stimulate BAT, even in obese mice resistant to the anorexic effects of leptin (21). Surprisingly, however, a role for NPY, acting via Y1R, in DMH control of BAT had not been previously investigated. Here we show that DMH NPY promptly suppresses cold-induced BAT activation, which appears to be mediated exclusively by the Y1R, since injection of BIBO3304 into the DMH reversed the effect of exogenous NPY. Thus, in hungry animals, increased NPY binding to Y1R in the DMH could override BAT thermogenesis triggered by cooling, to minimize energy expenditure. In addition, while SNA to BAT is typically undetectable or very low in anesthetized warmed rodents used to study its regulation, in individuals at subthermoneutral temperatures, such as rodents housed in vivarium temperatures, BAT SNA is likely ongoing. Therefore, fasting or hunger could suppress this ongoing activity via DMH Y1R. We also show that blockade of NPY Y1R in the DMH in warmed rats increases BAT SNA, indicating that tonically active NPY inputs into the DMH, via binding to Y1R, suppresses BAT SNA. Release of this tonic NPY inhibition of BAT SNA could contribute to the activation of BAT observed just prior to or with feeding, so-called diet- or feeding-induced thermogenesis (20, 22). Downstream, the DMH heavily innervates the RPa, which houses BAT premotor neurons involved in cooling and fever BAT activation. Our novel findings, that DMH NPY Y1R-expressing neuronal fibers were evident in the RPa, and that ArcN NPY/AgRP neurons closely associate with DMH-to-RPa neurons, provide anatomical substrates for functional links (in the control of BAT SNA) between the ArcN and RPa via DMH NPY-receptive neurons.

The present results confirm and extend previous reports (2, 8, 9) that PVN NPY inhibits BAT SNA, by showing in warmed rats that endogenous NPY tonically suppresses BAT SNA by binding to Y1R. Sensory detection of food and eating decreases ongoing ArcN NPY/AgRP activity (19). Therefore, a reduction in NPY release or Y1R activity in the PVN may also contribute to feeding-induced BAT activation. We also investigated potential downstream targets of PVN Y1R-expressing neurons that mediate NPY inhibition of BAT. A previous study suggested the following model (23): a key node is activation of GABAergic neurons in the IRt/PCRt that project to the RPa (11). Because PVN projections to the IRt/PCRt are sparse, it was proposed (23) that these GABAergic neurons are stimulated

indirectly. More specifically, in the PVN, NPY inhibits presynaptic release of GABA, thereby activating PVN output neurons, which are almost exclusively glutamatergic. These neurons in turn activate intermediate neurons in the NTS that project to and stimulate the GABAergic neurons in the IRt/PCRt. However, it is important to note that Y1R are largely postsynaptic, both anatomically and functionally (24–26). Instead, presynaptic inhibition of GABA release in the PVN is mediated more by Y2 and Y5 receptors (26). Our finding that PVN NPY Y1R containing neurons project directly to the RPa suggests a simpler model: NPY binding to postsynaptic Y1R inhibits PVN glutamatergic neurons that tonically drive the RPa. Further support of this model is that most PVN neurons that are capable of influencing BAT thermogenesis are surrounded by NPY terminals and are oxytocinergic (OT) (27). Moreover, ArcN NPY neurons synapse with PVN OT neurons (6), and OT neurons increase energy expenditure (28) via a direct connection to the RPa (29). Nevertheless, this simple model does not preclude additional, parallel circuitry, which includes the medullary IRt/PCRt, potentially mediated by PVN presynaptic NPY Y2R. Moreover, the extensive projection of PVN Y1R expressing neurons to the NTS may also influence BAT SNA via this integrating center.

It is well-established that ArcN NPY neurons are major players in the physiological adjustments to hunger or starvation, via projections to the PVN and DMH. However, most NPY inputs to the PVN arise from brainstem catecholaminergic (CA) neurons [largely from the ventrolateral medulla (VLM)] (30, 31); VLM CA/NPY neurons also project to the DMH (32–34). Under some circumstances, like lactation and obesity, NPY expression can become detectible in DMH neurons that project to the PVN (35, 36). Thus, NPY originating from these cohorts could also inhibit thermogenesis. Indeed, VLM glucose-sensing neurons mediate many homeostatic responses to glucoprivation, including decreases in BAT SNA and increases in food intake and the plasma levels of glucose and corticoids (37, 38). Furthermore, downregulation of VLM NPY and CA expression (but not either alone) suppresses glucoprivic feeding (39). However, PVN lesions do not impair the feeding response to low glucose, suggesting that VLM NPY/CA inputs to the PVN are not required for this response (37). Nevertheless, as previously hypothesized (30, 38), VLM CA/NPY inputs to the PVN may mediate the decreases in BAT SNA and temperature in response to glucoprivation (via either NPY postsynaptic Y1 or presynaptic Y2 receptors). Brainstem NPY projections to the DMH could also be involved in this and other glucoprivic responses. Clearly, further research is required to test and quantify the role of brainstem NPY inputs to the PVN and DMH in the regulation of energy balance, including BAT SNA and energy expenditure.

While the focus of this set of experiments was on NPY control of BAT SNA, we also provide information related to NPY inhibition of cardiovascularly relevant SNA via actions in the DMH and PVN. In the PVN, NPY has been previously shown to inhibit lumbar SNA, renal SNA, SSNA, MAP, HR (7, 16), as well as BAT SNA (8, 11) (Figure 4). In the DMH, blockade of NPY Y1R increases MAP, HR, and SSNA (7) (Figure 7). The DMH, like the PVN, is an integrative hub for the control of many modalities, including energy expenditure (BAT), respiration, and the cardiovascular system (10, 40, 41), as well as changes in these entities with psychological stress or challenges to in energy balance. Our studies, utilizing nanoinjections of NPY and BIBO3304 into the DMH, effect broad activation and inhibition

of the Y1R, which likely do not mimic the pattern of changes that might occur with various stresses to homeostasis. Thus, while NPY via Y1R in DMH influences the activity of many sympathetic nerves, patterned or varying responses may occur, depending on the stress or challenge. Indeed, previous studies have shown a topographic control of various efferents within the DMH (42, 43).

The present study provides some information regarding the downstream neurocircuity by which DMH and PVN NPY Y1R inhibit cardiovascularly-related SNA. In the DMH, the BIBO3304-induced increase in SSNA was reversed by blockade of the PVN. Given that DMH neurons that express NPY Y1R project heavily to the PVN (Figure 6), one interpretation of this finding is that disinhibition of DMH Y1R neurons increases SSNA via a neuronal pathway that includes the PVN. Alternatively, the PVN may provide the excitatory drive that mediates the increase in SSNA following release of tonic NPY Y1R inhibition of the DMH. In the PVN, in rats, Y1R are expressed in a small fraction (5–10%) of neurons that project to the RVLM, a major brainstem presympathetic hub (16). Therefore, we concluded that PVN NPY may decrease lumbar SNA via this direct projection. However, in the present study in mice, only modest numbers of fibers/nerve endings from PVN Y1R-expressing neurons were detected in the RVLM. Instead, a marked cluster of fibers and endings were evident in a brainstem region that may correspond to the caudal pressor area of the rat (17, 18), suggesting that at least in mice, PVN NPY may also inhibit SNA via this projection.

In conclusion, we show that DMH NPY inhibits BAT SNA in cooled rats via Y1R and that, in warmed animals with little ongoing BAT SNA, endogenous NPY binds to Y1R in both the DMH and PVN to tonically suppress BAT SNA and temperature. It appears that direct projections of NPY Y1R-expressing neurons in the DMH/PVN to the RPa are sufficient to mediate these responses, but other circuitry that includes additional medullary or hypothalamic nodes may be engaged in parallel or under different physiological or pathophysiological conditions. ArcN NPY neurons that project to the DMH and PVN are inhibited or stimulated by hormones intimately involved in energy balance in a sexually dimorphic manner, such as leptin, insulin, ghrelin, and estrogen. Therefore, release of tonic NPY Y1R inhibition may contribute to feeding- or diet-induced thermogenesis, whereas in hungry animals, increased NPY release could suppress BAT SNA under basal conditions or when provoked by cooling or infection. These data highlight the potential for the use of NPY1R antagonists to activate BAT and increase energy expenditure in obese individuals or in humans wishing to maintain weight loss.

ACKNOWLEDGEMENTS.

The authors are grateful to Dr. Brian Jenkins in the Advanced Light Microscopic Core (funded in part by P30 NS061800—PI Dr. Sue Aicher) for ihc image production.

FUNDING SOURCES.

This work was supported in part by NIH grant HL128181.

REFERENCES

1. Krashes MJ, Koda S, Ye C, Rogan SC, Adams AC, Cusher DS, Maratos-Flier E, Roth BL, Lowell BB. Rapid, reversible activation of AgRP neurons drives feeding behavior in mice. JClinInvest. 2011; 121(4): 1424–8.
2. Shi YC, Lau J, Lin Z, Zhang H, Zhai L, Sperk G, Heilbronn R, Mietzsch M, Weger S, Huang XF, Enriquez RF, Baldock PA, Zhang L, Sainsbury A, Herzog H, Lin S. Arcuate NPY controls sympathetic output and BAT function via a relay of tyrosine hydroxylase neurons in the PVN. Cell Metab. 2013; 17(2): 236–48. [PubMed: 23395170]
3. Vella KR, Ramadoss P, Lam FS, Harris JC, Ye FD, Same PD, O'Neill NF, Maratos-Flier E, Hollenberg AN. NPY and MC4R signaling regulate thyroid hormone levels during fasting through both central and peripheral pathways. Cell Metab. 2011; 14(6): 780–90. [PubMed: 22100407]
4. Patel HR, Qi Y, Hawkins EJ, Hileman SM, Elmquist JK, Imai Y, Ahima RS. Neuropeptide Y deficiency attenuates responses to fasting and high-fat diet in obesity-prone mice. Diabetes. 2006; 55(11): 3091–8. [PubMed: 17065347]
5. Zhang L, Ip CK, Lee IJ, Qi Y, Reed F, Karl T, Low JK, Enriquez RF, Lee NJ, Baldock PA, Herzog H. Diet-induced adaptive thermogenesis requires neuropeptide FF receptor-2 signalling. Nature communications. 2018; 9(1): 4722.
6. Atasoy D, Betley JN, Su HH, Sternson SM. Deconstruction of a neural circuit for hunger. Nature. 2012; 488(7410): 172–7. [PubMed: 22801496]
7. Shi Z, Madden CJ, Brooks VL. Arcuate neuropeptide Y inhibits sympathetic nerve activity via multiple neuropathways. J Clin Invest. 2017; 127(7): 2868–80. [PubMed: 28628036]
8. Egawa M, Yoshimatsu H, Bray GA. Neuropeptide Y suppresses sympathetic activity to interscapular brown adipose tissue in rats. Am J Physiol. 1991; 260(2 Pt 2): R328–34. [PubMed: 1996720]
9. Kotz CM, Briggs JE, Grace MK, Levine AS, Billington CJ. Divergence of the feeding and thermogenic pathways influenced by NPY in the hypothalamic PVN of the rat. Am J Physiol. 1998; 275(2): R471–7. [PubMed: 9688682]
10. Morrison SF, Nakamura K. Central Mechanisms for Thermoregulation. Annu Rev Physiol. 2019; 81285–308. [PubMed: 30256726]
11. Nakamura Y, Yanagawa Y, Morrison SF, Nakamura K. Medullary Reticular Neurons Mediate Neuropeptide Y-Induced Metabolic Inhibition and Mastication. Cell Metab. 2017.
12. Padilla SL, Qiu J, Soden ME, Sanz E, Nestor CC, Barker FD, Quintana A, Zweifel LS, Ronnekleiv OK, Kelly MJ, Palmiter RD. Agouti-related peptide neural circuits mediate adaptive behaviors in the starved state. Nat Neurosci. 2016; 19(5): 734–41. [PubMed: 27019015]
13. Shi Z, Pelletier NE, Wong J, Li B, Sdrulla AD, Madden CJ, Marks DL, Brooks VL. Leptin increases sympathetic nerve activity via induction of its own receptor in the paraventricular nucleus. eLife. 2020; 9.
14. Li B, Shi Z, Cassaglia PA, Brooks VL. Leptin acts in the forebrain to differentially influence baroreflex control of lumbar, renal, and splanchnic sympathetic nerve activity and heart rate. Hypertension. 2013; 61(4): 812–9. [PubMed: 23424232]
15. Shi Z, Cassaglia PA, Pelletier NE, Brooks VL. Sex differences in the sympathoexcitatory response to insulin in obese rats: role of neuropeptide Y. J Physiol. 2019; 597(6): 1757–75. [PubMed: 30628058]
16. Cassaglia PA, Shi Z, Li B, Reis WL, Clute-Reinig NM, Stern JE, Brooks VL. Neuropeptide Y acts in the paraventricular nucleus to suppress sympathetic nerve activity and its baroreflex regulation. JPhysiol. 2014; 592(Pt 7): 1655–75. [PubMed: 24535439]
17. Campos RR, Carillo BA, Oliveira-Sales EB, Silva AM, Silva NF, Futuro Neto HA, Bergamaschi CT. Role of the caudal pressor area in the regulation of sympathetic vasomotor tone. Braz J Med Biol Res. 2008; 41(7): 557–62. [PubMed: 18719736]
18. Sun W, Panneton WM. The caudal pressor area of the rat: its precise location and projections to the ventrolateral medulla. Am J Physiol Regul Integr Comp Physiol. 2002; 283(3): R768–78. [PubMed: 12185012]
19. Chen Y, Lin YC, Kuo TW, Knight ZA. Sensory detection of food rapidly modulates arcuate feeding circuits. Cell. 2015; 160(5): 829–41. [PubMed: 25703096]

20. Blessing WW. Thermoregulation and the ultradian basic rest-activity cycle. Handb Clin Neurol. 2018; 156367–75. [PubMed: 30454601]
21. Enriori PJ, Sinnayah P, Simonds SE, Garcia RC, Cowley MA. Leptin action in the dorsomedial hypothalamus increases sympathetic tone to brown adipose tissue in spite of systemic leptin resistance. JNeurosci. 2011; 31(34): 12189–97. [PubMed: 21865462]
22. van Marken Lichtenbelt WD, Schrauwen P. Implications of nonshivering thermogenesis for energy balance regulation in humans. Am J Physiol Regul Integr Comp Physiol. 2011; 301(2): R285–96. [PubMed: 21490370]
23. Nakamura K, Nakamura Y. Hunger and Satiety Signaling: Modeling Two Hypothalamomedullary Pathways for Energy Homeostasis. Bioessays. 2018; 40(8): e1700252. [PubMed: 29869415]
24. Eva C, Serra M, Mele P, Panzica G, Oberto A. Physiology and gene regulation of the brain NPY Y1 receptor. Front Neuroendocrinol. 2006; 27(3): 308–39. [PubMed: 16989896]
25. Thorsell A, Mathé AA. Neuropeptide Y in Alcohol Addiction and Affective Disorders. Front Endocrinol (Lausanne). 2017; 8178. [PubMed: 28824541]
26. Pronchuk N, Beck-Sickinger AG, Colmers WF. Multiple NPY receptors Inhibit GABA(A) synaptic responses of rat medial parvocellular effector neurons in the hypothalamic paraventricular nucleus. Endocrinology. 2002; 143(2): 535–43. [PubMed: 11796508]
27. Oldfield BJ, Giles ME, Watson A, Anderson C, Colvill LM, McKinley MJ. The neurochemical characterisation of hypothalamic pathways projecting polysynaptically to brown adipose tissue in the rat. Neuroscience. 2002; 110(3): 515–26. [PubMed: 11906790]
28. Lawson EA, Olszewski PK, Weller A, Blevins JE. The role of oxytocin in regulation of appetitive behaviour, body weight and glucose homeostasis. J Neuroendocrinol. 2019e12805. [PubMed: 31657509]
29. Fukushima AN K Oxytocinergic neurons in the hypothalamic paraventricular nucleus stimulate brown adipose tissue thermogenesis through rostral medullary raphe. FASEB J. 2019; 33850.6.
30. Guyenet PG, Stornetta RL, Bochorishvili G, Depuy SD, Burke PG, Abbott SB. C1 neurons: the body's EMTs. Am J Physiol Regul Integr Comp Physiol. 2013; 305(3): R187–204. [PubMed: 23697799]
31. Füzesi T, Wittmann G, Liposits Z, Lechan RM, Fekete C. Contribution of noradrenergic and adrenergic cell groups of the brainstem and agouti-related protein-synthesizing neurons of the arcuate nucleus to neuropeptide-y innervation of corticotropin-releasing hormone neurons in hypothalamic paraventricular nucleus of the rat. Endocrinology. 2007; 148(11): 5442–50. [PubMed: 17690163]
32. Woulfe JM, Flumerfelt BA, Hrycyshyn AW. Efferent connections of the A1 noradrenergic cell group: a DBH immunohistochemical and PHA-L anterograde tracing study. Exp Neurol. 1990; 109(3): 308–22. [PubMed: 1976532]
33. Abbott SB, DePuy SD, Nguyen T, Coates MB, Stornetta RL, Guyenet PG. Selective optogenetic activation of rostral ventrolateral medullary catecholaminergic neurons produces cardiorespiratory stimulation in conscious mice. J Neurosci. 2013; 33(7): 3164–77. [PubMed: 23407970]
34. Stornetta RL, Akey PJ, Guyenet PG. Location and electrophysiological characterization of rostral medullary adrenergic neurons that contain neuropeptide Y mRNA in rat medulla. JComp Neurol. 1999; 415(4): 482–500. [PubMed: 10570457]
35. Lee SJ, Kirigiti M, Lindsley SR, Loche A, Madden CJ, Morrison SF, Smith MS, Grove KL. Efferent projections of neuropeptide Y-expressing neurons of the dorsomedial hypothalamus in chronic hyperphagic models. JComp Neurol. 2013; 521(8): 1891–914. [PubMed: 23172177]
36. Bi S Dorsomedial hypothalamic NPY modulation of adiposity and thermogenesis. Physiol Behav. 2013; 12156–60. [PubMed: 23562863]
37. Ritter S, Li AJ, Wang Q. Hindbrain glucoregulatory mechanisms: Critical role of catecholamine neurons in the ventrolateral medulla. Physiol Behav. 2019; 208112568. [PubMed: 31173784]
38. Madden CJ. Glucoprivation in the ventrolateral medulla decreases brown adipose tissue sympathetic nerve activity by decreasing the activity of neurons in raphe pallidus. AmJPhysiol RegulIntegrComp Physiol. 2012; 302(2): R224–R32.

39. Li AJ, Wang Q, Dinh TT, Ritter S. Simultaneous silencing of Npy and Dbh expression in hindbrain A1/C1 catecholamine cells suppresses glucoprivic feeding. J Neurosci. 2009; 29(1): 280–7. [PubMed: 19129404]

40. Fontes MA, Xavier CH, de Menezes RC, Dimicco JA. The dorsomedial hypothalamus and the central pathways involved in the cardiovascular response to emotional stress. Neuroscience. 2011; 18464–74. [PubMed: 21435377]

41. Fukushi I, Yokota S, Okada Y. The role of the hypothalamus in modulation of respiration. Respir Physiol Neurobiol. 2019; 265172–9. [PubMed: 30009993]

42. Tanaka M, McAllen RM. Functional topography of the dorsomedial hypothalamus. Am J Physiol Regul Integr Comp Physiol. 2008; 294(2): R477–86. [PubMed: 18077509]

43. Cao WH, Fan W, Morrison SF. Medullary pathways mediating specific sympathetic responses to activation of dorsomedial hypothalamus. Neuroscience. 2004; 126(1): 229–40. [PubMed: 15145088]

44. Paxinos G, Watson C. The rat brain in sterotaxic coordinates San Diego: Academic Press, 2007.

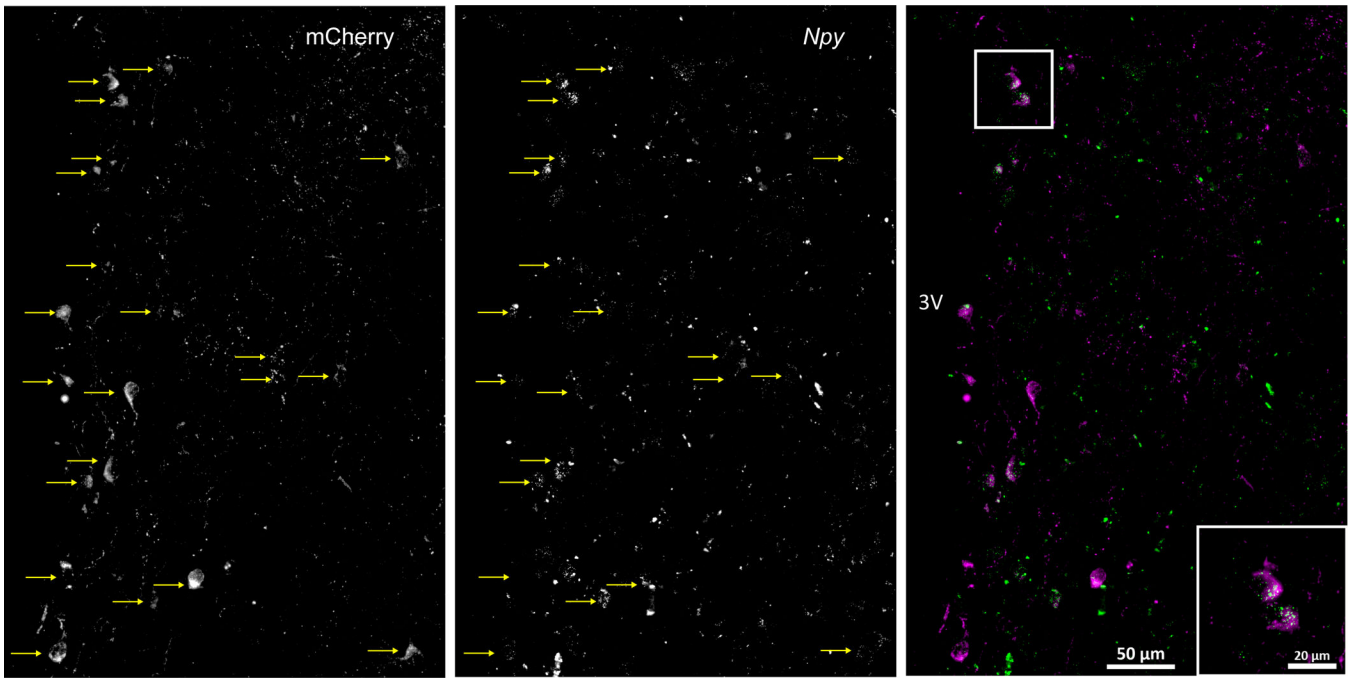

Fig. 1. Selective expression of AAV-Syn-mCherry in neurons that express Npy1r.

Male *npy1*r-*cre* mice received unilateral PVN injections of a *cre*-dependent adeno-associated virus (AAV), allowing for the selective expression of a fluorescent protein (mCherry; left panel) in synaptosomes, which can be visualized in the cell bodies, axon fibers, and synapses of NPY Y1R-containing neurons (middle panel). Images show that 95% (19/20) of neurons that expressed mCherry (magenta) also expressed mRNA for the NPY1R (green puncta; at least 3 per neuron), quantified using RNAScope (right panel).

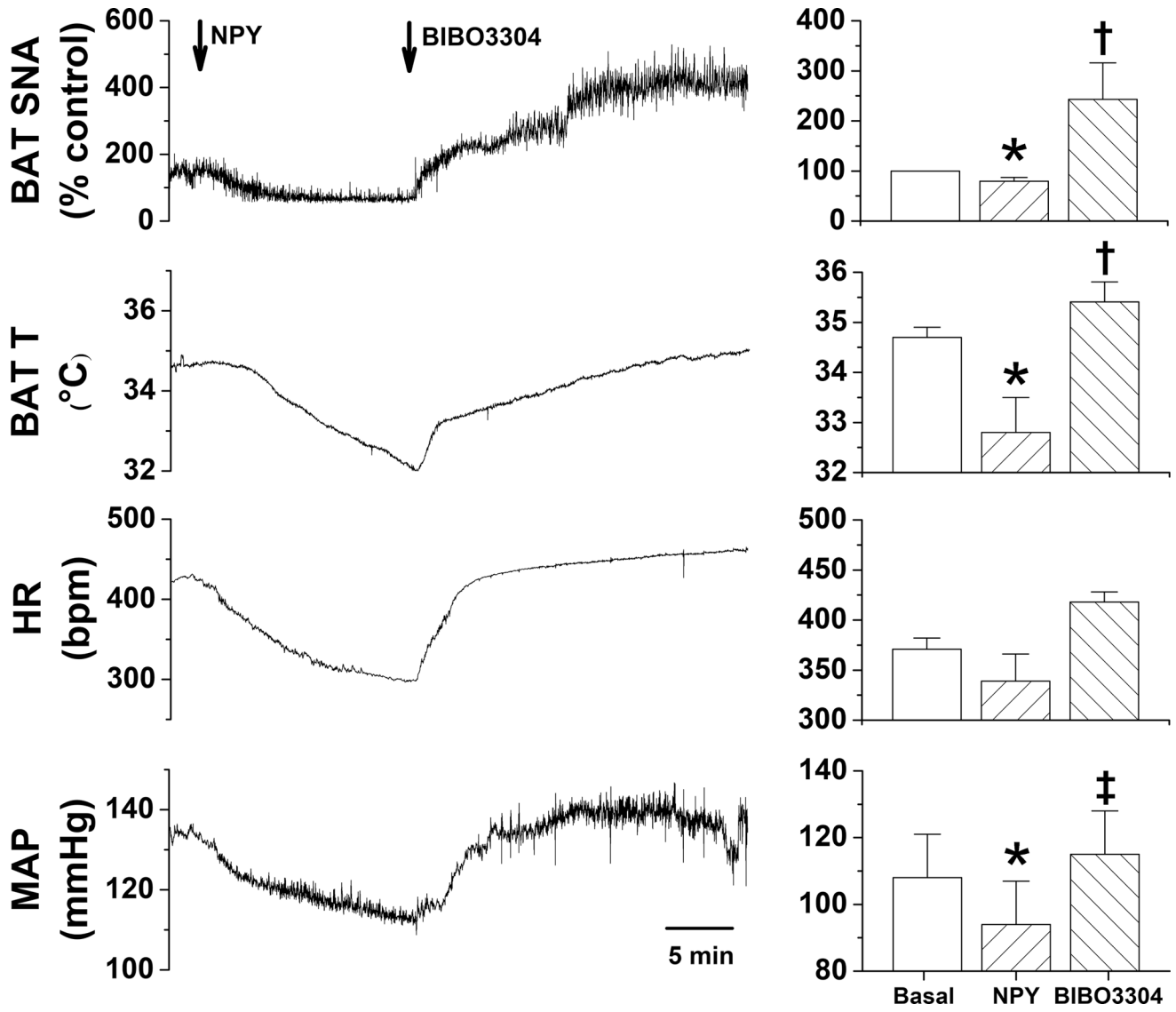

Fig. 2. In cooled rats, bilateral nanoinjections of NPY into the DMH decreases BAT SNA, and this inhibition is reversed by subsequent blockade of NPY Y1R, with BIBO3304.

Left, representative experiment. Right, grouped data (n=3). 1-way repeated measures ANOVA revealed significant changes in BAT SNA [F=35.7 (2,4), P<0.005], BAT temperature [F=32.6 (2,4), P<0.005], MAP [F=9.1 (2,4), P<0.05], but not HR (F=3.73 (2,4), P>0.05]. *: P<0.05, compared to basal. †: P<0.05, compared to basal and NPY. ‡: P<0.05 compared to NPY.

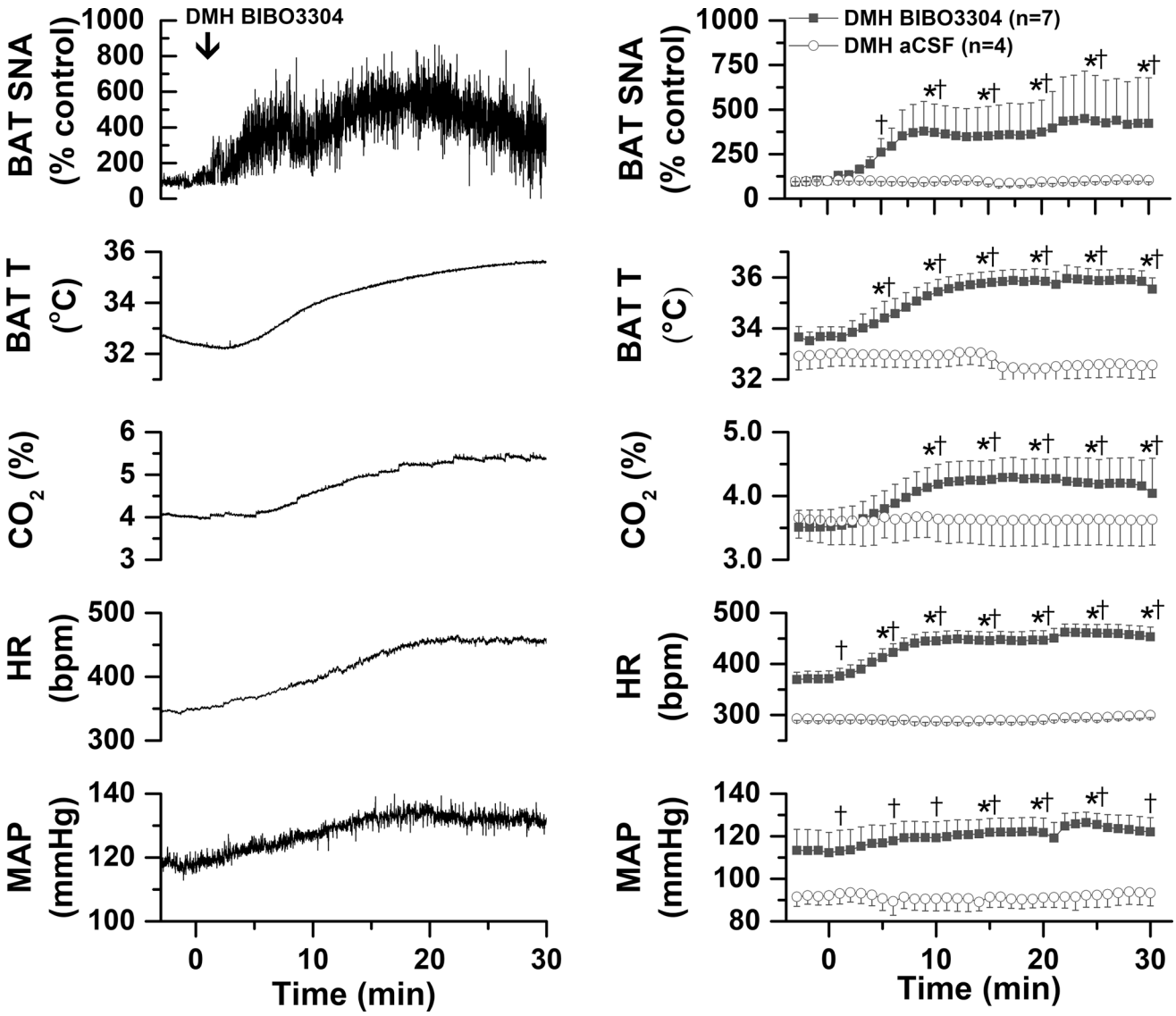

Fig. 3. In warmed rats, blockade of DMH NPY Y1R with BIBO3304 increases BAT SNA and temperature, expired CO_2, MAP, and HR.

Left, representative experiment. Right, grouped data for rats that received BIBO3304 (n=7) or aCSF (n=4). Two-way ANOVA for repeated measures was conducted on the time course every 5 min. The analysis revealed significant changes in BAT SNA [F_{group}=29.4 (1,9), P<0.05; F_{time}=3.5 (6,66), P<0.01; $F_{interaction}$=4.13 (6,54), P<0.005]; BAT temperature [F_{group}=23.3 (1,9), P<0.001; F_{time}=5.6 (6,66), P<0.0005; $F_{interaction}$=4.13 (6,66), P<0.005]; CO_2 [F_{group}=0.17 (1,9), P>0.10; F_{time}=5.5 (6,66), P<0.0005; $F_{interaction}$=4.26 (6,66), P<0.005; HR [F_{group}=59.5 (1,9), P<0.0001; F_{time}=4.7 (6,66), P<0.001; $F_{interaction}$=4.17 (6,66), P<0.005]; and MAP [F_{group}=8.2 (1,9), P<0.05; F_{time}=0.92 (6,66), P>0.10; $F_{interaction}$=0.87 (6,66), P>0.10]. *: P<0.05, compared to basal. †: P<0.05, between group difference.

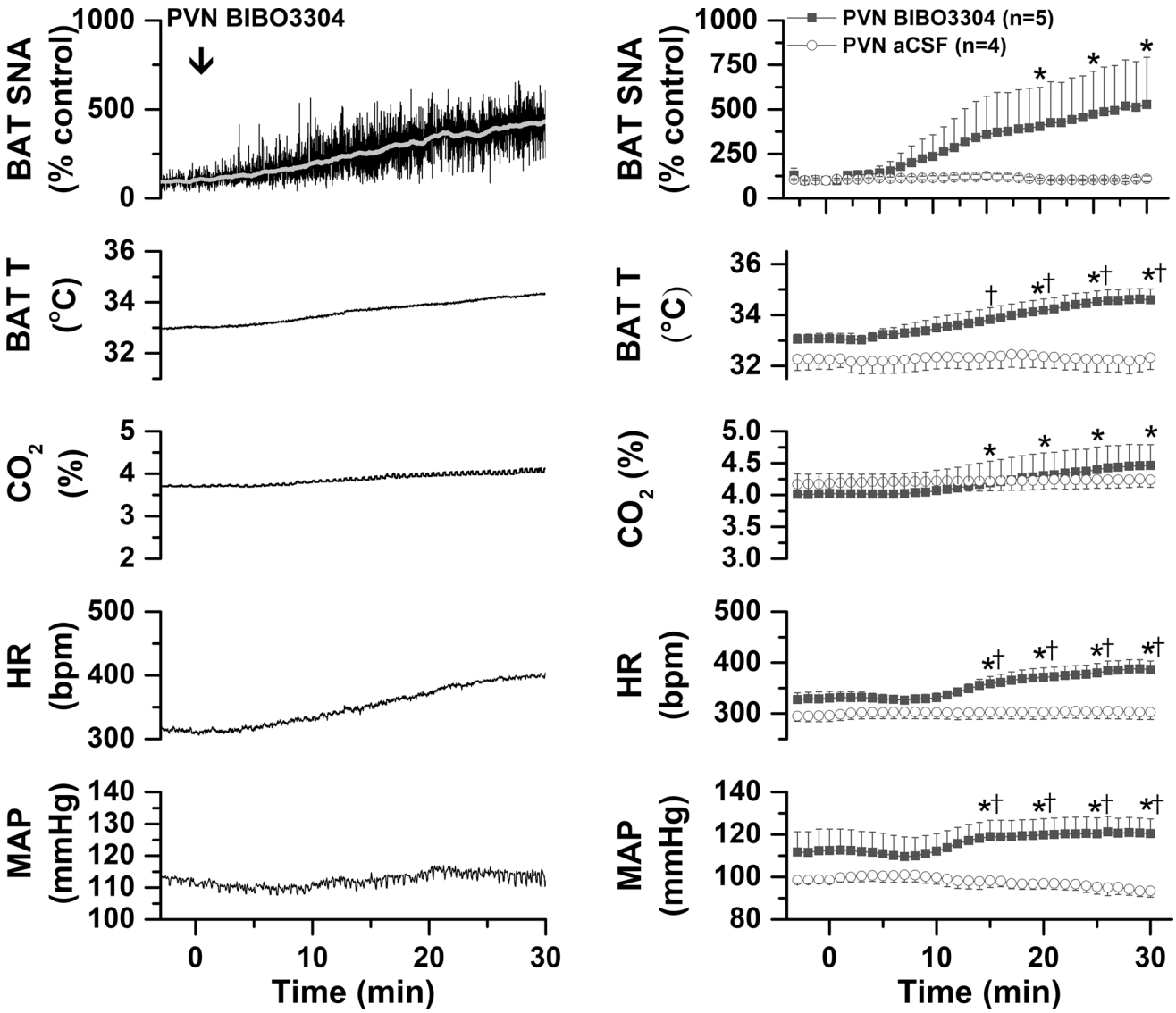

Fig. 4. In warmed rats, blockade of PVN NPY Y1R with BIBO3304 increases BAT SNA and temperature, expired CO_2, MAP, and HR.

Left, representative experiment. Right, grouped data for rats that received BIBO3304 (n=5) or aCSF (n=4). Two-way ANOVA for repeated measures was conducted on the time course every 5 min. The analysis revealed significant changes in BAT SNA [F_{group}=5.8 (1,7), P<0.05; F_{time}=2.4 (6,42), P<0.05; $F_{interaction}$=4.45 (6,42), P<0.005]; BAT temperature [F_{group}=7.8 (1,7), P<0.05; F_{time}=5.7 (6,42), P<0.0005; $F_{interaction}$=4.26 (6,42), P<0.005]; CO_2 [F_{group}<0.1 (1,7), P>0.10; F_{time}=11.1 (6, 2), P<0.0001; $F_{interaction}$=7.27 (6,42), P<0.0001; HR [F_{group}=10.2 (1,7), P<0.05; F_{time}=4.4 (6,42), P<0.005; $F_{interaction}$=3.56 (6,42), P<0.01]; and MAP [F_{group}=4.13 (1,7), P<0.10; F_{time}=0.62 (6,42), P>0.10; $F_{interaction}$=4.0 (6,42), P<0.005]. *: P<0.05, compared to basal. †: P<0.05, between group difference.

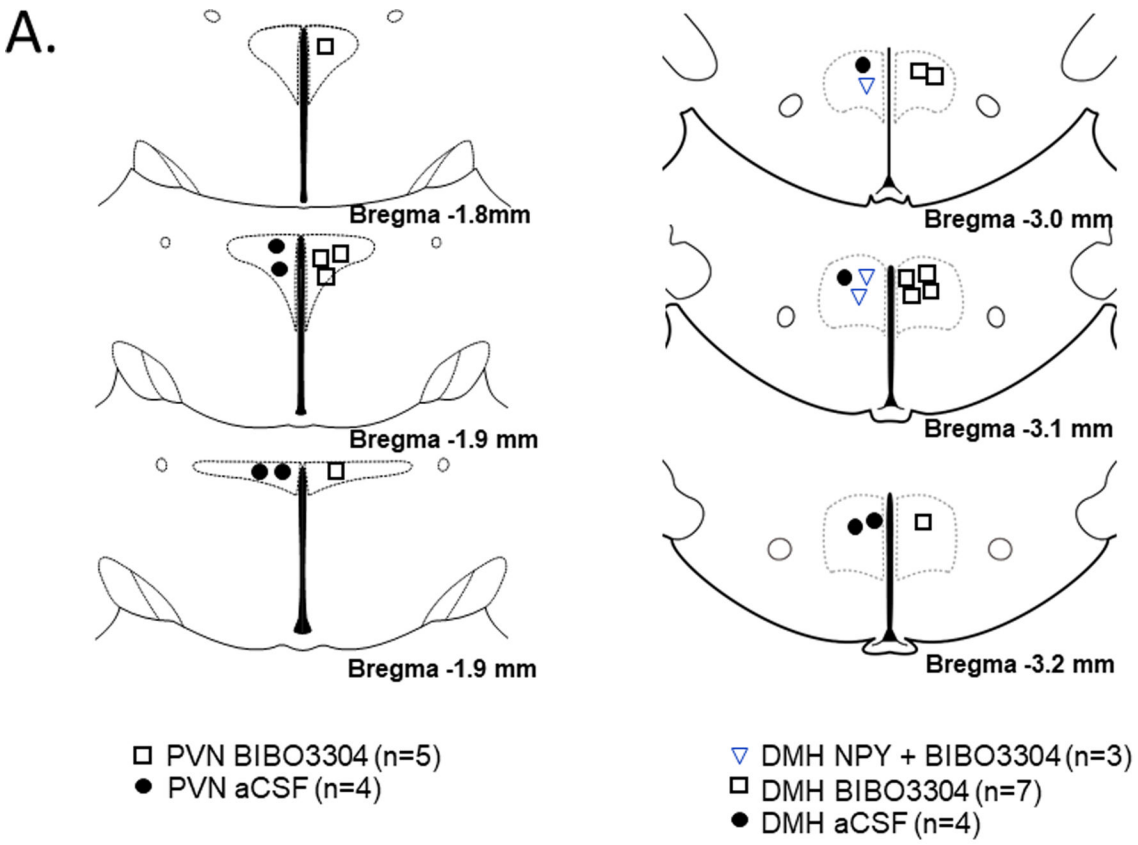

Fig. 5. Histological maps (A) and photomicrographs of nanoinjected fluorescent microspheres (B) illustrating DMH and PVN injection sites.

Histological images modified from (44).

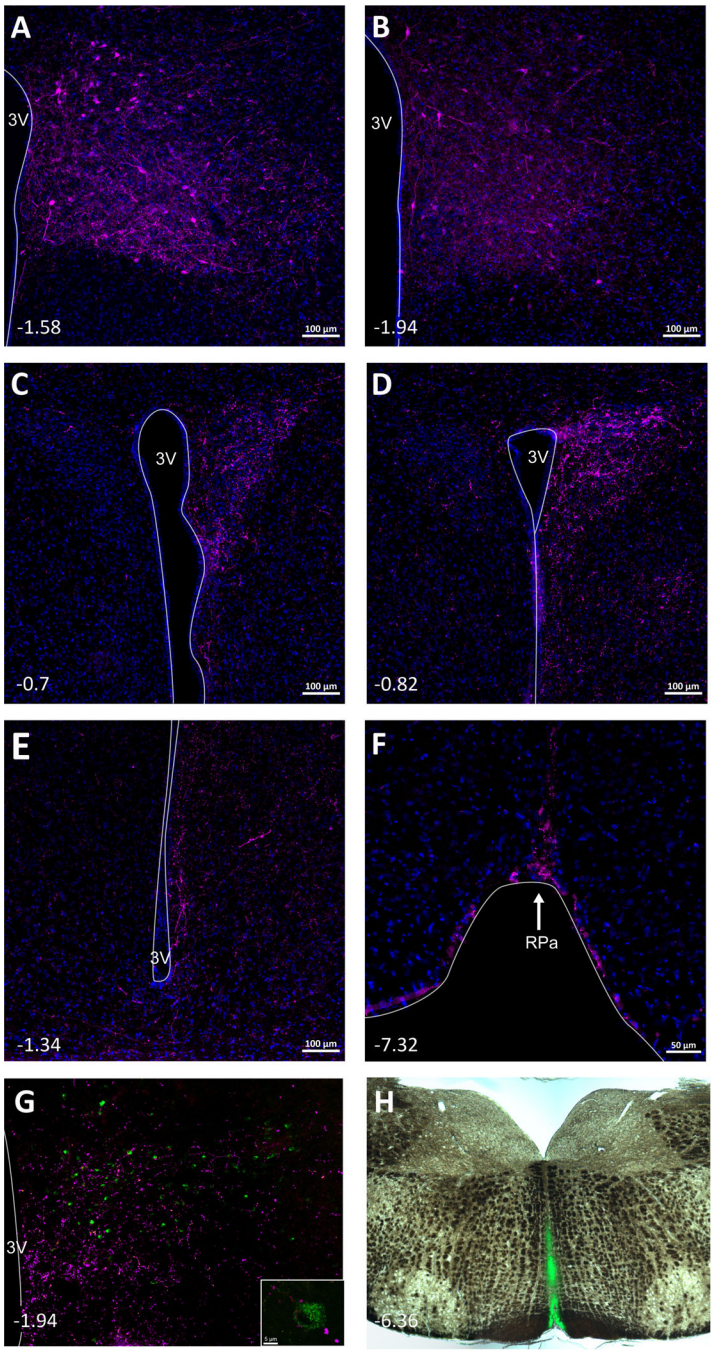

Fig. 6. DMH Y1R-expressing neurons project to the PVN, Raphe Pallidus (RPa), and ArcN.

A and B. Localized expression of mCherry in cell bodies in the DMH of *npyr1-cre* mice that received AAV-Syn-mCherry. **C and D.** Abundant mCherry fibers were found in the PVN. Fibers from DMH NPY Y1R-expressing neurons were also observed in the ArcN (**E**) and RPa (**F**). In the DMH, cell bodies that project to the RPa (**G**), visualized with injections of the retrograde tracer CtB (green) in the RPa (**H**), are closely associated with fibers (magenta) from ArcN NPY/AgRP neurons, as in inset, captured with confocal microscopy (63x) (images modified from (7)).

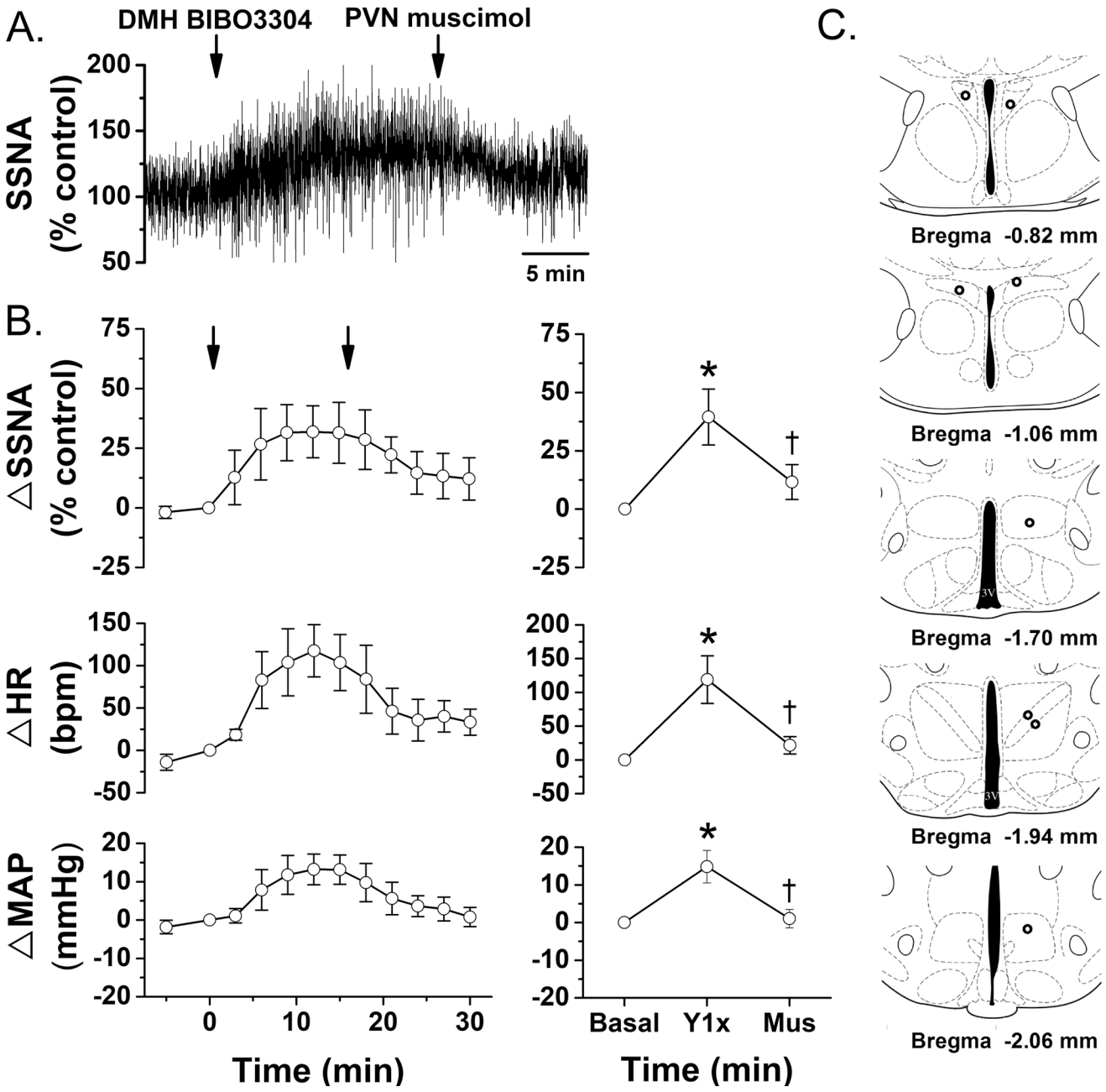

Fig. 7. In WT mice, blockade of DMH NPY Y1R with BIBO3304 (Y1x), increases SSNA, HR, and MAP, which is reversed by nonspecific blockade of the PVN with muscimol (Mus).

Left, time course. 1-way repeated measures ANOVA revealed a significance effect of time/treatment (P<0.05). **A.** Representative experiment. **B.** Grouped data (n=5), showing mean±SEM of peak responses after DMH BIBO3304 or PVN muscimol. 1-way repeated measures ANOVA revealed significant changes in SSNA [F=9.7 (2, 6), P<0.05], MAP [F=11.9 (2,6), P<0.01], and HR (F=6.3 (2,6), P<0.05]. **C.** Histological maps showing injection sites. *: P<0.05, compared to basal. †: P<0.05, difference between DMH Y1x and PVN muscimol.

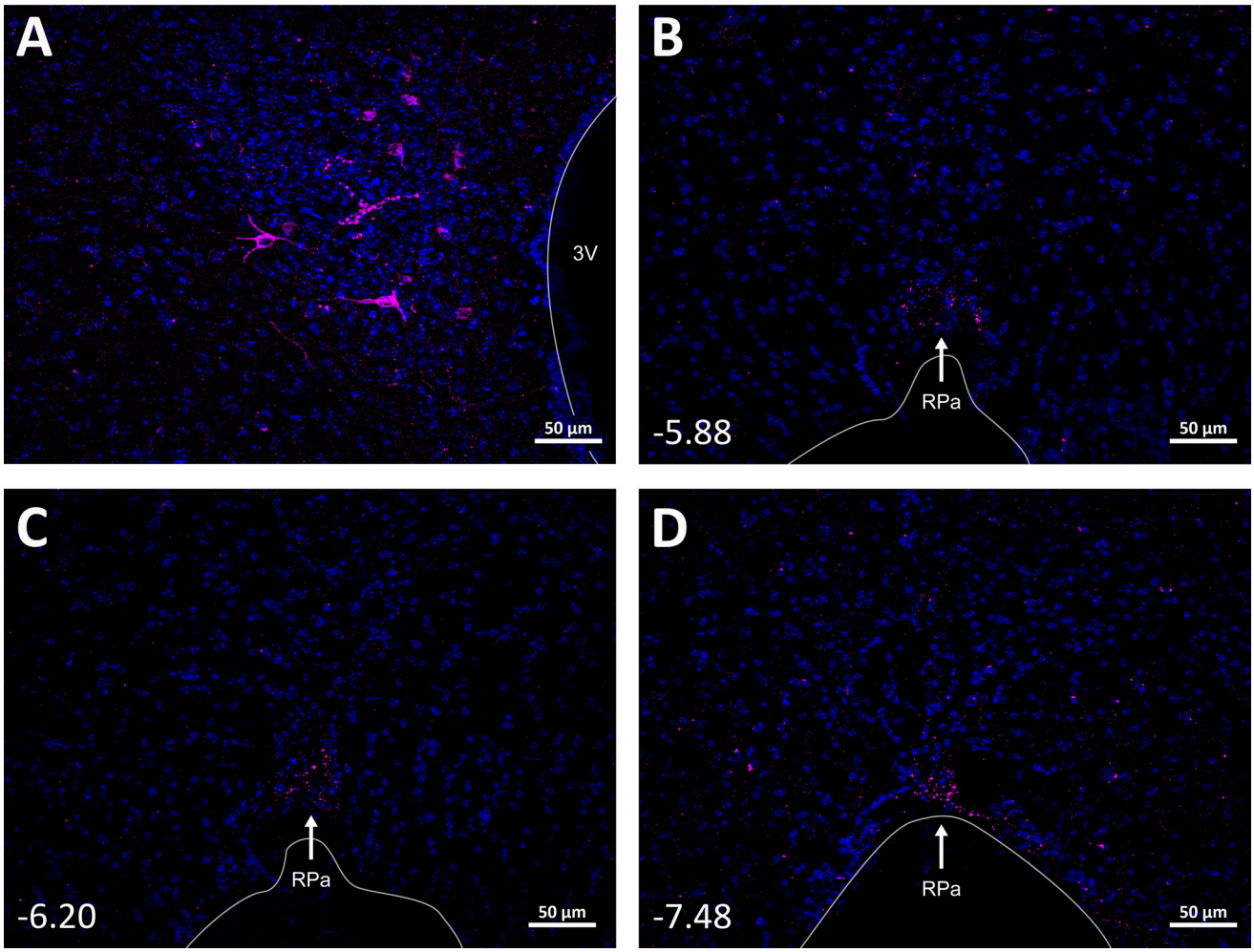

Fig. 8. PVN Y1R-expressing neurons project to the Raphe Pallidus (RPa).

A. Select expression of mCherry in PVN NPY1R neurons in a representative mouse (n=3). **B, C,** and **D**. mCherry fibers and nerve endings from PVN NPYR1 neurons were found throughout the rostral-caudal RPa.

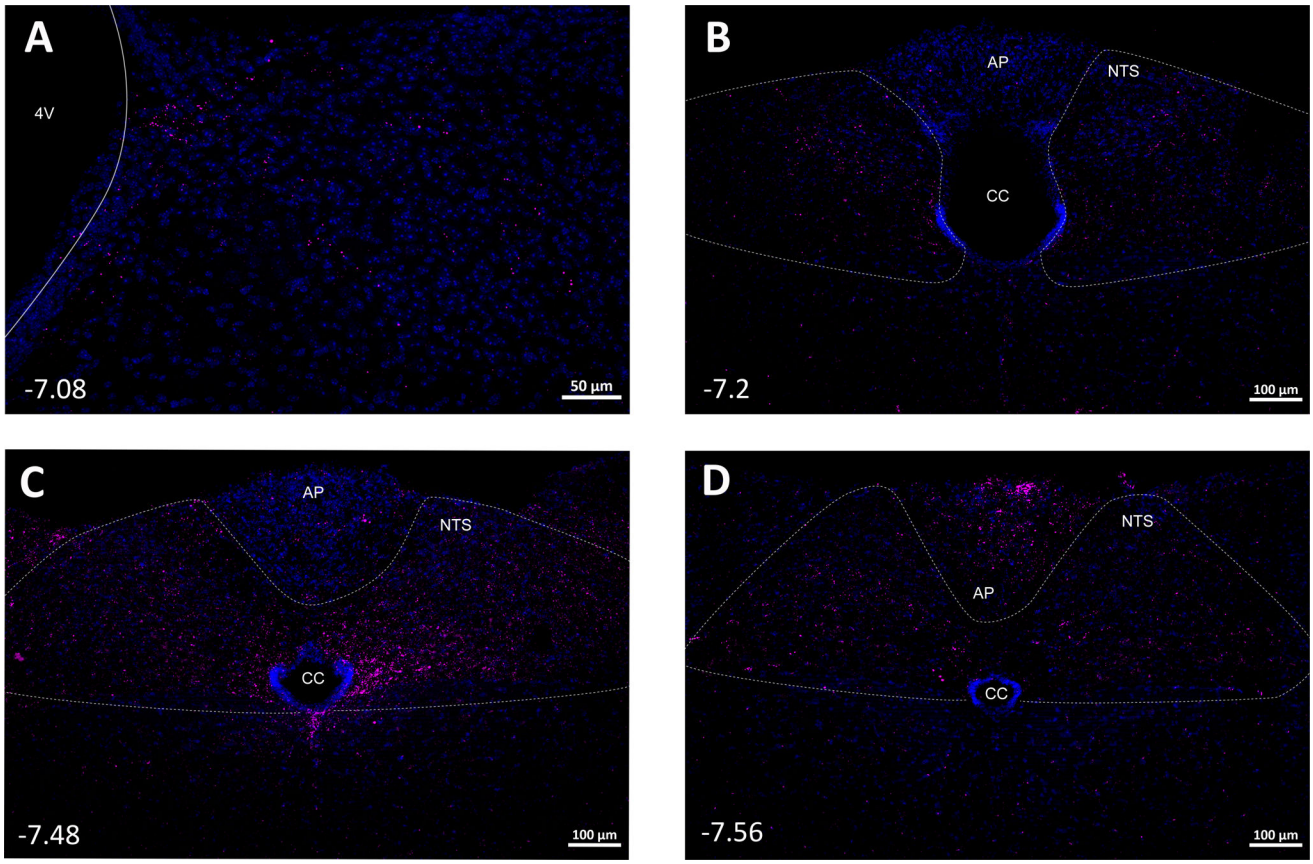

Fig. 9. Fibers from PVN Y1R-expressing neurons were found throughout the nucleus tractus solitarius (NTS) and area postrema (AP).

CC: central canal.

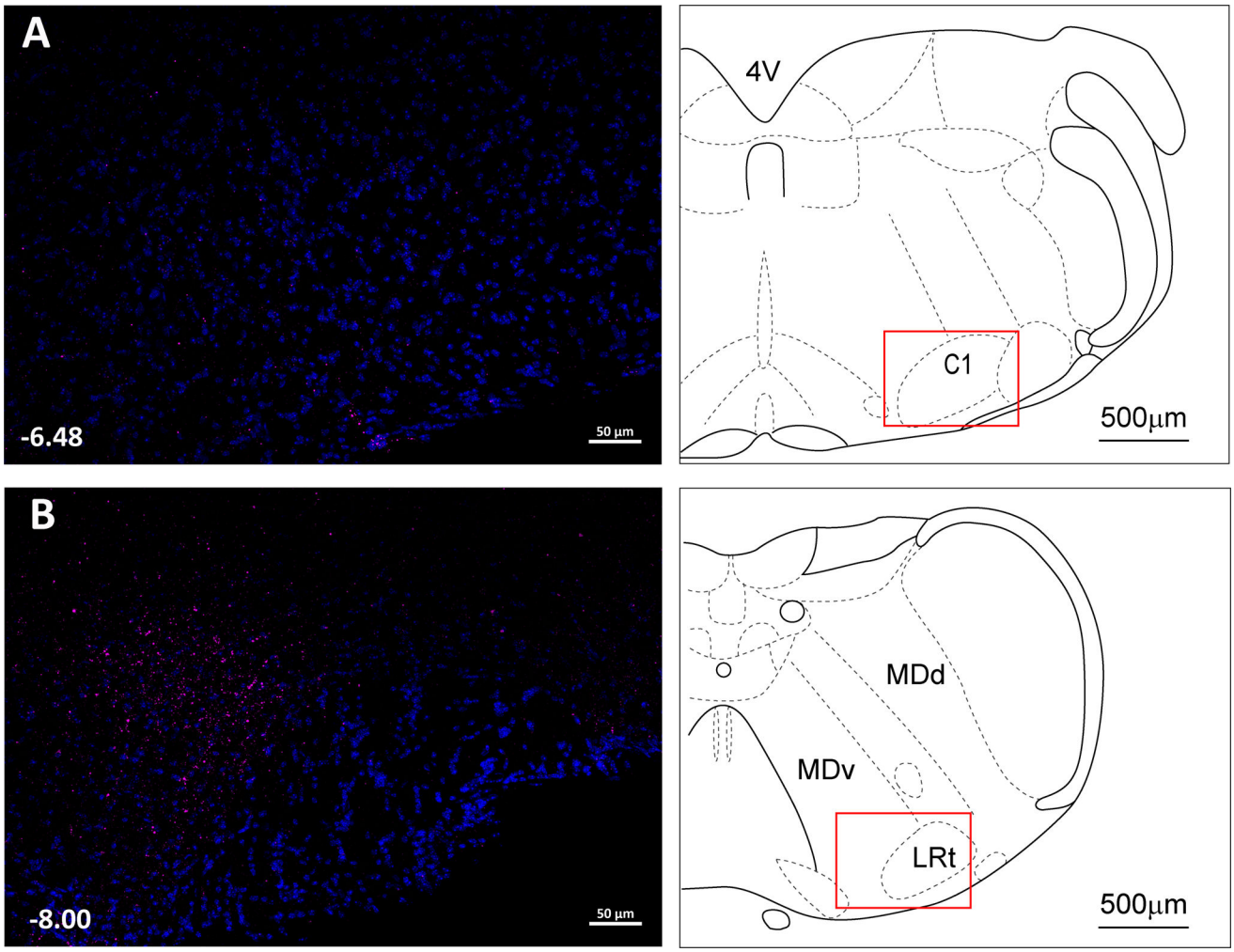

Fig. 10.
PVN Y1R-expressing neurons project to the RVLM (**A**) and presumed CPA (**B**).